LARGE DISPLACEMENT ANALYSIS OF LAMINATED BEAM-TYPE STRUCTURES

Igor Pešić[1*] – Goran Turkalj[2]

[1]Department of Polytechnics, University of Rijeka, Sveučilišna avenija 4, 51000 Rijeka, Croatia
[2]Department of Engineering Mechanics, Faculty of Engineering, University of Rijeka, Vukovarska 58, 51000 Rijeka, Croatia

ARTICLE INFO

***Article history*:**
Received: 04.04.2023.
Received in revised form: 12.05.2023.
Accepted: 16.05.2023.

Keywords:
Beam
Stability
Buckling
Composite
Laminate
Non-linear analysis

DOI: https://doi.org/10.30765/er.2184

Abstract:

The paper presents a finite element formulation for analysis of 3D framed structures with thin-walled laminated composite cross-sections, using a co-rotational approach. The formulation considers the effects of large displacements on the response of space frames subjected to conservative and static external loads. Classical lamination theory for thin fiber-reinforced laminates has been employed. Stability analysis is performed in load deflection manner using co-rotational formulation. The shear strain of the middle surface is assumed to be zero, and the cross-section is not distorted in its own plane. In order to illustrate the application of the proposed formulation, several numerical examples are presented.

1 Introduction

Composite materials have gained significant attention in recent years due to their high strength-to-weight ratio, corrosion resistance, and excellent fatigue properties. Composite laminated spatial beams, which are commonly used in aerospace and civil engineering applications, offer significant advantages over their metallic counterparts in terms of weight reduction and design flexibility. However, these structures are susceptible to various types of instability, including buckling, vibration, and flutter. Therefore, it is crucial to ensure the global stability of these structures under different loading conditions. Large displacement analysis is an essential tool for predicting the load-carrying capacity of composite laminated spatial beams and ensuring their structural integrity. Numerous papers have been dedicated to performing finite element buckling analysis on various types of composite beams, and only a selection of these papers is referenced here. Lee and Kim [1] have studied flexural–torsional buckling of thin-walled I-section composites. Kim et al. [2] have proposed numerical method to evaluate exactly the element stiffness matrix for the lateral buckling analysis of thin-walled composite I- and channel-section beams with symmetric and arbitrary laminations subjected to end moments.

Vo and Lee have presented geometrically nonlinear model for composite box beams [3] and general thin-walled open-section composite beams [4] with arbitrary lay-ups under various types of loadings. That model accounts for all structural coupling coming from the material anisotropy and geometric nonlinearity and nonlinear governing equations are derived and solved by means of an incremental Newton–Raphson method. Silvestre, Camotim and their co-workers [5]-[7] introduced a second-order Generalised Beam Theory (GBT) developed to analyse the buckling behaviour of composite thin-walled members which incorporates both local and global deformation modes. Saravia et al. [8] have presented geometrically nonlinear beam finite element for composite closed section thin-walled beams considering arbitrary displacements and rotations. Ahmadi and Rasheed [9] have developed generalized semi-analytical approach for lateral-torsional buckling of simply supported anisotropic, thin-walled, rectangular cross-section beams under concentrated load at mid-span/mid-height.

* Corresponding author
E-mail address:igor.pesic@uniri.hr

Huang and Qiao [10], [11] have presented semi-analytical solution for critical buckling load and nonlinear load-deflection relationship of I-section laminated composite curved beams with elastic end restraints. They derived the governing differential equations of thin-walled curved beams from the principle of virtual displacement with full consideration of curvature effect. Banić et al. [12] have presented shear deformable beam model for the nonlinear stability analysis of composite beam-type structures. The model derives incremental equilibrium equations in the framework of an updated Lagrangian formulation. Stability analysis is a crucial aspect in the design and analysis of load-carrying structures. Two approaches are commonly used for this purpose: eigenvalue analysis [13] and load-deflection analysis [14]. The former approach neglects pre-buckling deformations, while the latter considers the entire range of loading, including pre-buckling and post-buckling phases. The load-deflection analysis, also known as nonlinear stability analysis, is more reliable for imperfect or real structures and loading conditions with or without material nonlinearity.

Nonlinear response of load-carrying structures requires numerical methods such as the finite element method. Different descriptions, such as the total and updated Lagrangian ones [15], [16], and the co-rotational description [17] - [20] can be utilized. The co-rotational description is a well-known approach for developing efficient beam elements for nonlinear analysis of structures. It is linear on the element level, and geometrically nonlinear effects are introduced through the transformation from the local coordinate system to the global one. In this paper co-rotational description is used to develop a finite element formulation for stability analysis of 3D framed structures with thin-walled laminated composite cross-section. The formulation considers the effects of large displacements on the response of space frames subjected to conservative and static external loads. Classical lamination theory for thin fiber-reinforced laminates has been employed, and the formulation is applicable to any arbitrary laminate cross-section shape. The shear strain of the middle surface is assumed to be zero, and the cross-section is not distorted in its own plane.

2 Theoretical background

2.1 Kinematics

In a local Cartesian coordinate system in which beam axis, that connects all cross sectional centres of gravity, coincides with *z* axis while *x* and *y* are principal axes, cross sectional rigid body displacements are:

$$\begin{aligned} &w_0 = w_0(z), \quad u_0 = u_0(z), \quad v_0 = v_0(z), \\ &\phi_z = \phi_z(z), \quad \phi_x = -\frac{dv_0}{dz}, \quad \phi_y = \frac{du_0}{dz}, \\ &\theta = -\frac{d\phi_z}{dz}. \end{aligned} \tag{1}$$

In Eq. (1), w_o, u_o and v_o are the rigid body translations in the *z*-, *x*- and *y*-directions, respectively; ϕ_z, ϕ_x and ϕ_y are the rigid body rotations around *z*-, *x*- and *y*-axes, respectively, while θ is a cross-sectional warping parameter. The displacement components of an arbitrary point of the cross section are defined as:

$$\begin{aligned} &w = w_o - y\frac{dv_0}{dz} - x\frac{du_0}{dz} - \omega\frac{d\phi_z}{dz} \\ &u = u_o - y\ \phi_z \\ &v = v_o + x\ \phi_z \end{aligned} \tag{2}$$

where *x* and *y* define the position of the cross section, while ω is a value of the cross-sectional warping function. The strain tensor components can be written as:

$$\varepsilon_z = \frac{dw_o}{dz} - y\frac{d\phi_x}{dz} - x\frac{d\phi_y}{dz} - \omega\frac{d^2\phi_z}{dz^2} + \frac{1}{2}(x^2+y^2)\left(\frac{d\phi_z}{dz}\right)^2 \tag{3}$$

$$\varepsilon_{zs} = 2n\frac{d\phi_z}{dz} \tag{4}$$

where s is a circumferential coordinate and n is a normal coordinate in a coordinate system which is introduced into the middle contour of the cross section.

2.2 Ply stress and strains

Figure 1 shows an orthotropic unidirectionally reinforced lamina whose in-plane principal material axes are aligned to the natural plate axes z and s.

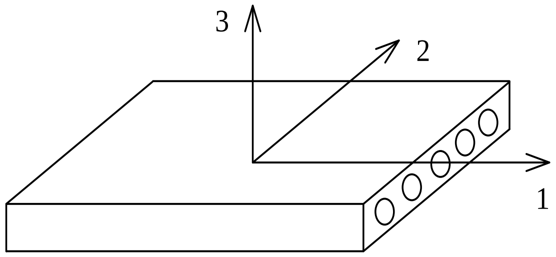

Figure 1. Unidirectionally reinforced lamina.

The stress-strain relations for plane stress on the orthotropic lamina in principal material coordinates are:

$$\begin{Bmatrix} \sigma_1 \\ \sigma_2 \\ \tau_{12} \end{Bmatrix} = \begin{bmatrix} Q_{11} & Q_{12} & 0 \\ Q_{12} & Q_{22} & 0 \\ 0 & 0 & Q_{66} \end{bmatrix} \begin{Bmatrix} \varepsilon_1 \\ \varepsilon_2 \\ \gamma_{12} \end{Bmatrix} \tag{5}$$

Where the lamina reduced stiffnesses in terms of the engineering constants are:

$$\begin{gathered} Q_{11} = \frac{E_1}{1-\nu_{12}\nu_{21}}, \; Q_{22} = \frac{E_2}{1-\nu_{12}\nu_{21}}, \\ Q_{12} = \frac{\nu_{12}E_2}{1-\nu_{12}\nu_{21}} = \frac{\nu_{21}E_2}{1-\nu_{12}\nu_{21}}, \; Q_{66} = G_{12} \end{gathered} \tag{6}$$

In Figure 2, an elementary volume is shown with principal axes 1 and 2. To obtain the stress resultants of a beam cross-section, it is necessary to perform a transformation from the coordinate system of the material's principal axes (1-2) to the natural plate axes (z–s). The fibers are oriented at an angle of θ with respect to the positive direction of the z-axis. The positive direction of the angle θ is chosen in the direction opposite to the clockwise rotation.

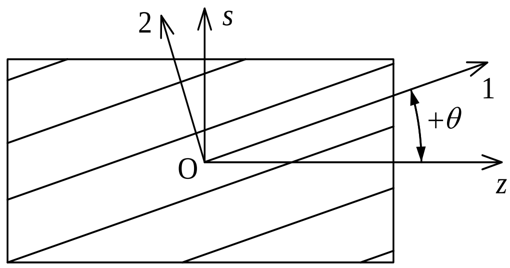

Figure 2. Lamina in the natural plate coordinate system.

After the transformation the stresses in laminate coordinates are:

$$\begin{Bmatrix} \sigma_z \\ \sigma_s \\ \tau_{zs} \end{Bmatrix} = \begin{bmatrix} \bar{Q}_{11} & \bar{Q}_{12} & \bar{Q}_{16} \\ \bar{Q}_{12} & \bar{Q}_{22} & \bar{Q}_{26} \\ \bar{Q}_{16} & \bar{Q}_{26} & \bar{Q}_{66} \end{bmatrix} \begin{Bmatrix} \varepsilon_z \\ \varepsilon_s \\ \gamma_{zs} \end{Bmatrix} \tag{7}$$

Where the lamina transformed reduced stiffnesses are:

$$\begin{aligned}
\bar{Q}_{11} &= Q_{11}\cos^4\theta + 2(Q_{12}+2Q_{66})\sin^2\theta\cos^2\theta + Q_{22}\sin^4\theta \\
\bar{Q}_{22} &= Q_{11}\sin^4\theta + 2(Q_{12}+2Q_{66})\sin^2\theta\cos^2\theta + Q_{22}\cos^4\theta \\
\bar{Q}_{16} &= (Q_{11}-Q_{12}-2Q_{66})\sin\theta\cos^3\theta + (Q_{12}-Q_{22}+2Q_{66})\cos\theta\sin^3\theta \\
\bar{Q}_{66} &= (Q_{11}+Q_{22}-2Q_{12})\sin^2\theta\cos^2\theta + Q_{66}\left(\cos^2\theta-\sin^2\theta\right)^2 \\
\bar{Q}_{12} &= (Q_{11}+Q_{22}-4Q_{66})\sin^2\theta\cos^2\theta + Q_{12}\left(\cos^4\theta+\sin^4\theta\right) \\
\bar{Q}_{26} &= (Q_{11}-Q_{12}-2Q_{66})\cos\theta\sin^3\theta + (Q_{12}-Q_{22}+2Q_{66})\sin\theta\cos^3\theta
\end{aligned} \tag{8}$$

After assumption that the transverse normal stresses are insignificant ($\sigma_s = 0$), the constitutive equations are:

$$\begin{Bmatrix}\sigma_z \\ \tau_{zs}\end{Bmatrix} = \begin{bmatrix}\bar{Q}^*_{11} & \bar{Q}^*{}_{16} \\ \bar{Q}^*{}_{16} & \bar{Q}^*{}_{66}\end{bmatrix}\begin{Bmatrix}\varepsilon_z \\ \gamma_{zs}\end{Bmatrix} \tag{9}$$

Where the transformed reduced stiffness coefficients are:

$$\begin{aligned}
\bar{Q}^*_{11} &= \bar{Q}_{11} - \frac{\bar{Q}_{12}{}^2}{\bar{Q}_{22}} \\
\bar{Q}^*_{16} &= \bar{Q}_{16} - \frac{\bar{Q}_{12}\bar{Q}_{16}}{\bar{Q}_{22}} \\
\bar{Q}^*_{66} &= \bar{Q}_{66} - \frac{\bar{Q}_{26}{}^2}{\bar{Q}_{22}}
\end{aligned} \tag{10}$$

Integrating over the laminate thickness *n* and the contour direction *s*, and transforming into the beam coordinate system, the cross-sectional internal force components follow:

$$\begin{aligned}
&F_z = \int_A \sigma_z dA \ , \quad M_x = \int_A \sigma_z y dA \, , \\
&M_y = -\int_A \sigma_z x dA \, , \quad M_z = \int_A \tau_{zs}\, n dA, \\
&M_\omega = \int_A \sigma_z \omega dA \, , \quad T_\sigma = \int_A \sigma_z (x^2+y^2) dA
\end{aligned} \tag{11}$$

where F_z represents the axial force, M_z is the torsion moment, M_x and M_y are bending moments with respect to the *x* and *y* axes, respectively, M_ω is the bimoment and T_σ is the Wagner coefficient.
The shear forces F_x and F_y are treated as the reactive ones and can be determined as the first derivative of bending moments M_y and M_x with respect to *z*-coordinate, respectively.

2.3 Beam finite element

In Figure 3 two-nodded beam finite element with eight degrees of freedom is presented:

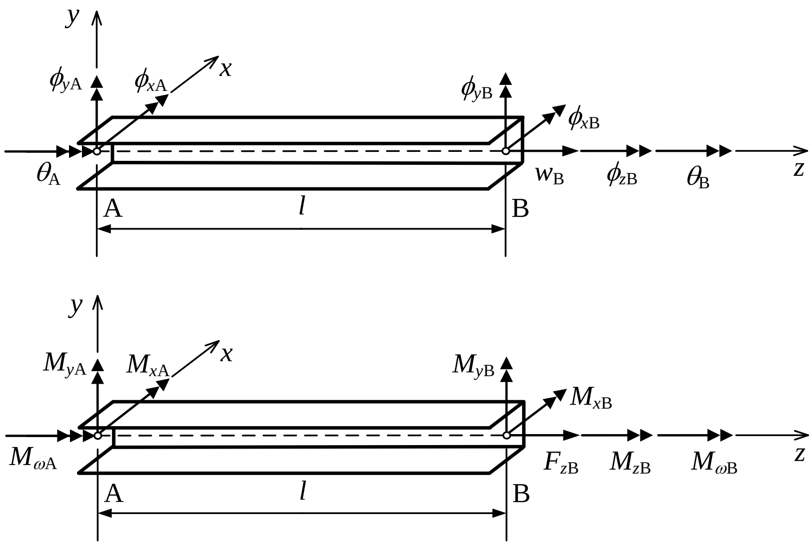

Figure 3. Two-nodded spatial beam element in local coordinate system.

The nodal displacement vector of the beam element is:

$$(\mathbf{u}^e)^{\mathrm{T}} = \{w_{\mathrm{B}}, \phi_{z\mathrm{B}}, \phi_{x\mathrm{A}}, \phi_{x\mathrm{B}}, \phi_{y\mathrm{A}}, \phi_{y\mathrm{B}}, \theta_{\mathrm{A},}, \theta_{\mathrm{B}}\} \tag{12}$$

An appropriate nodal force vector is:

$$(\mathbf{f}^e)^{\mathrm{T}} = \{F_{z\mathrm{B}}, M_{z\mathrm{B}}, M_{x\mathrm{A}}, M_{x\mathrm{B}}, M_{y\mathrm{A}}, M_{y\mathrm{B}}, M_{\omega\mathrm{A}}, M_{\omega\mathrm{B}}\} \tag{13}$$

Incremental analysis supposes that a load-deflection path is subdivided into a number of steps or increments. This path is usually described using three configurations: the initial or undeformed configuration C_0; the last calculated equilibrium configuration C_1 and current unknown configuration C_2. Adopting co-rotational formulation, all system quantities should be referred to configuration C_2. Applying the virtual work principle and neglecting the body forces, the equilibrium of a finite element can be expressed as:

$$\delta U = \delta W \tag{14}$$

in which U is potential energy of internal forces, W is the virtual work of external forces, while δ denotes virtual quantities. After making the first variation of Eq. (11), the following incremental equations can be obtained:

$$\delta W = (\delta \mathbf{u}^e)^{\mathrm{T}}\, \mathbf{f}^e\,; \qquad \delta U = (\delta \mathbf{u}^e)^{\mathrm{T}}\, \mathbf{k}_{\mathrm{T}}^e\, \mathbf{u}^e \tag{15}$$

In Eq. (15), $\mathbf{k}_{\mathrm{T}}^e$ denotes the tangent stiffness matrix of the e-th beam element in the local coordinate system, and which is obtained according to the procedure presented in Ref. [21]. Now, the incremental equilibrium equation of the element can be written in the following form:

$$\mathbf{k}_{\mathrm{T}}^e\, \Delta \mathbf{u}^e = \Delta \mathbf{f}^e \tag{16}$$

The three-points Gaussian integration is made in the direction of element length, while the integration over a cross-section area is performed by subdividing the cross section into a finite number of monitoring areas, Figure 4.

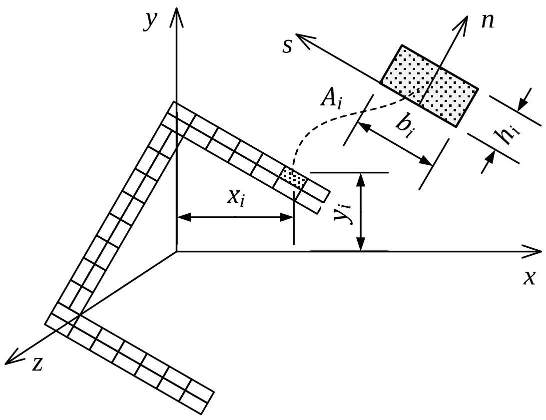

Figure 4. Cross-sectional discretization.

In Figure 4, a channel cross-section subdivided into a finite number of monitoring areas $\Delta A_i = b_i \times h_i$, each defined by coordinates x_i and y_i of the pertaining centroid, is shown. After summing up all the monitoring areas, the internal force components of the cross-section at Gaussian points can be obtained as:

$$\begin{aligned} F_z(z) &= \sum_{i=1}^{m} \sigma_{zi}\, \Delta A_i\,, \quad M_x(z) = \sum_{i=1}^{m} \sigma_{zi}\, y_i\, \Delta A_i\,, \quad M_y(z) = -\sum_{i=1}^{m} \sigma_{zi}\, x\, \Delta A_i\,, \\ M_z(z) &= \sum_{i=1}^{m} \tau_{zsi} n_i\, \Delta A_i\,, \quad M_\omega(z) = \sum_{i=1}^{m} \sigma_{zi}\, \omega_i\, \Delta A_i\,, \quad T_\sigma(z) = \sum_{i=1}^{m} \sigma_{zi}\left(x_i^2 + y_i^2\right) \Delta A_i, \end{aligned} \tag{17}$$

where the index m denotes the total number of monitoring areas.

2.4 Local to global system transformation

To transform the tangent stiffness matrix of each beam element into the global coordinate system, the nonlinear transformation procedure from Ref. [17], accounting for the large rotation effects, is adopted in this study, i.e.

$$\bar{\mathbf{k}}_{\mathrm{T}}^{e} = \mathbf{t}_1^{e}\, \mathbf{k}_{\mathrm{T}}^{e}\, \mathbf{t}_1^{e} + \mathbf{t}_2^{e}\, \mathbf{f}^{e}. \tag{18}$$

In Eq. (18), $\mathbf{t}_1^e$ is a transformation matrix of dimension 14×8, which contains the first derivatives of element displacements in the local coordinate system with respect to the global ones, while $\mathbf{t}_2^e$ is a transformation matrix of dimension 14×14×8 and contains the second derivatives of element displacements. The matrix $\mathbf{t}_2^e$ occur due to the change in structural geometry and reflects its effects on the global forces. The element force vector is transformed from the local to global coordinate system as:

$$\bar{\mathbf{f}}^{e} = \mathbf{t}_1^{e}\, \mathbf{f}^{e}. \tag{19}$$

After performing the standard assembling procedure, the overall incremental equilibrium equations can be obtained as:

$$\mathbf{K_T}\, \mathbf{U} = \mathbf{P}, \quad \mathbf{K_T} = \sum_e \bar{\mathbf{k}}_{\mathbf{T}}^{e}, \quad \mathbf{P} = {}^2\mathbf{P} - {}^1\mathbf{P}. \tag{20}$$

where $\mathbf{K}_{\mathrm{T}}$ is tangential stiffness matrix of a structure, while $\mathbf{U}$ and $\mathbf{P}$ are the incremental displacement vector and the incremental external loads of the structure, respectively. The vectors ${}^2\mathbf{P}$ and ${}^1\mathbf{P}$ denote the external loads applied to a structure at the new and last calculated configurations, respectively.

3 Results and discussion

The nonlinear finite element algorithm presented above is implemented in a computer program called *Eulam*. The generalized displacement control method has been employed as an incremental-iterative solution scheme. The updating of nodal coordinates as well as orientations of the cross-sections and axes of each element is performed at the end of each iteration. Because of the non-commutative character of large incremental nodal orientations, the updating of nodal orientations for a new deformed configuration is performed using Rodriguez' large rotation formula [22]. The effectiveness of the algorithm is validated through several test examples.

3.1 Bending and twisting of a console

A channel cantilever of length L = 2 m, shown in Figure 5, is loaded with a transverse force F through the centroid of the free end cross-section. The cantilever is modelled with a single finite element. The channel cross-section is composed of four layers of S2-glass/epoxy composite with following material characteristics: E_1 = 48.3 GPa, E_2 = 19.8 GPa, G_{12} = 8.96 GPa and ν_{12} = 0.27.

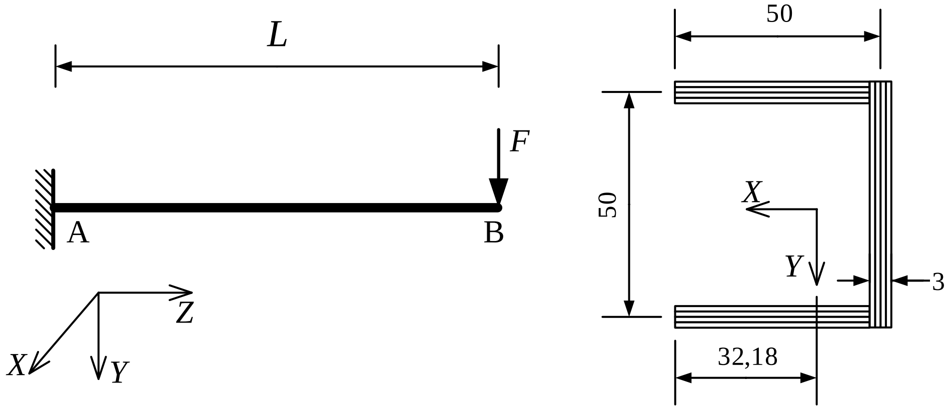

Figure 5. Channel cantilever under a transverse load.

Two cases of laminate stacking were considered: $[0]_4$ and $[45/-45]_s$. Figure 6 shows a comparison of the obtained results with those reported by Cardoso et al. [23], who used eight beam finite elements.

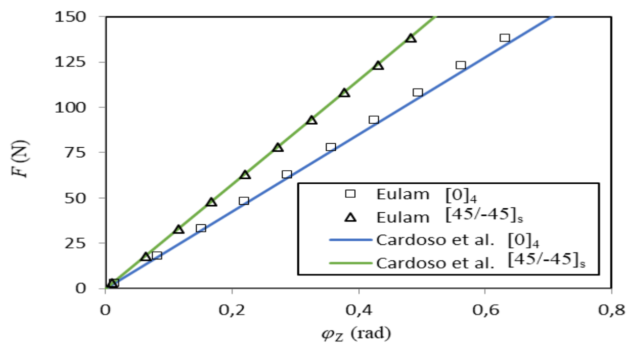

Figure 6. Load vs. twisting of the cantilever free end.

3.2 Lateral-torsional buckling of right-angle frame

Figure 7 shows a simply supported right-angle frame subjected to a single concentrated force F acting in the negative Y-axis direction. To initiate the occurrence of lateral-torsional buckling, a horizontal perturbation force □F=0,001F acting in the positive Z-axis direction is added at the corner B. A rectangular cross-section 30×0.6 mm is used for the two legs of the frame. Laminate is made of eight plies with stacking sequence $[0_8]$, $[□/90]_{2S}$ and $[90_8]$. The material properties E_1 = 140 GPa, E_2 = 10 GPa, G_{12} = 5 GPa and ν_{12} = 0.3 are used.

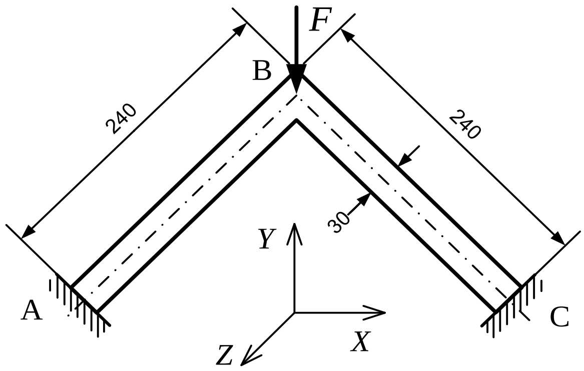

Figure 7. Simply supported right angle frame.

The lowest lateral-torsional buckling load for all the stacking sequence cases is obtained by an eigenvalue analysis in the computer program NASTRAN. Due to symmetry, only the left side of the frame has been idealised using 512 shell finite elements, and the lowest buckling mode is shown in Figure 8.

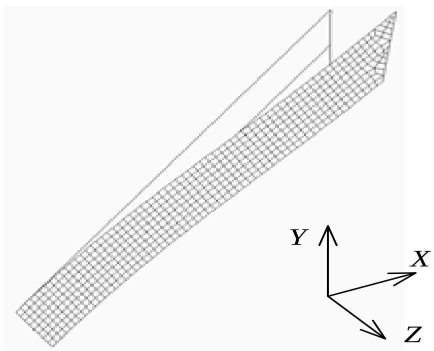

Figure 8. First buckling mode – shell model NASTRAN.

The obtained results for the lateral deflection of the corner B in the Z-axis direction are shown in Figure 9.

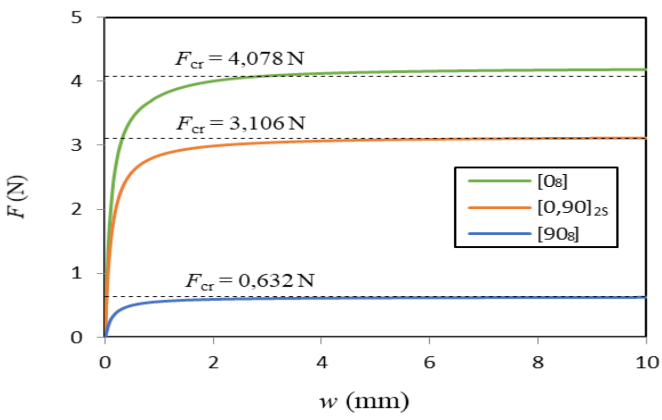

Figure 9. Load-deflection curves for different lamina orientation.

3.3 Sway buckling of one-story one-bay space frame

Figure 10 shows a one-story space frame loaded by four vertical forces, each of intensity F. To initiate the sway buckling mode, two perturbation forces ΔF = 0,001F acting in positive X-axis direction are added at corners A and D. All the frame members are made of two four layered laminates that form a cruciform cross section 200x200x10mm. The configuration of both laminates is $[\varphi/-\varphi]_s$. Analysed material is graphite-epoxy (AS4/3501) with the material properties: E_1 = 144 GPa, E_2 = 9.65 GPa, G_{12} = 4.14 GPa and ν_{12} = 0.26. Each frame leg is discretized by four beam finite elements of equal length.

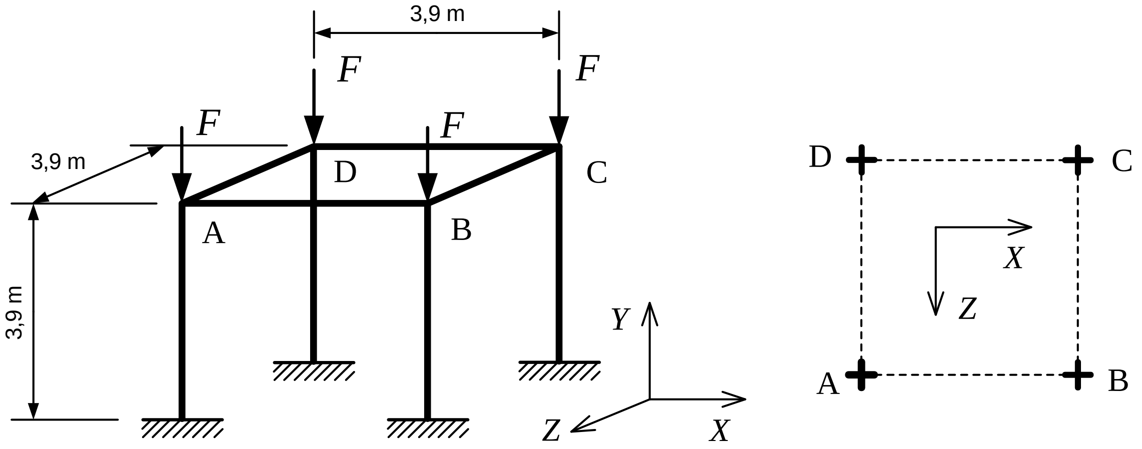

Figure 10. One-story space frame.

The buckling of the space frame for the fibre orientation in the range from 0° to 60° has been analysed. The critical buckling loads with linear shell model in Nastran using 4234 finite elements (Figure 11) have been determined. The nonlinear response for different lamina orientation together with critical buckling loads obtained by NASTRAN is presented in Figure 12.

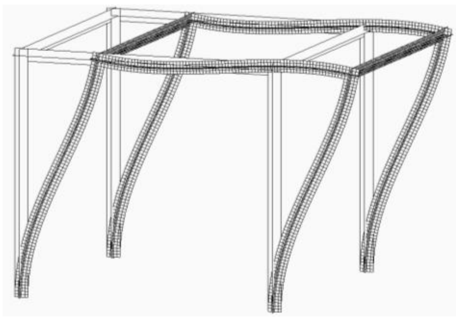

Figure 11. Sway buckling mode.

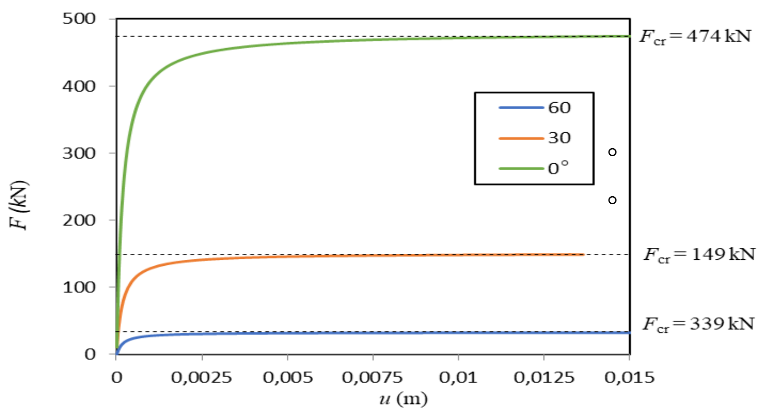

Figure 12. Load-deflection curves for different lamina orientation.

4 Conclusion

The co-rotational description has been utilized to develop a finite element formulation for the stability analysis of 3D framed structures with thin-walled laminated composite cross-section, which has considered the effects of large displacements on the response of space frames subjected to conservative and static external loads. This formulation is applicable to any arbitrary laminate cross-section shape and has been derived using classical lamination theory for thin fiber-reinforced laminates. The authors have presented verification examples to demonstrate the accuracy of the proposed formulation. The formulation has been found to be appropriate and efficient in analysing complex structural behaviour under a large rotation regime. Overall, the presented formulation and approach can be valuable for engineers and researchers in the field of stability analysis and could aid in predicting the load-carrying capacity of composite laminated spatial beams and ensure their structural integrity under different loading conditions

Acknowledgement:

The authors gratefully acknowledge financial support from Croatian Science Foundation (project No. IP-2019-04-8615) and University of Rijeka (uniri-tehnic-18-107).

References

[1] J. Lee and S.-E. Kim, "Flexural-torsional buckling of thin-walled I-section composites", Computers & Structures, vol. 79, no. 10, pp. 987-995, 2001. [Online]. Available: https://doi.org/10.1016/S0045-7949(00)00195-4.

[2] N. Kim, D. K. Shin, and M. Kim, "Exact lateral buckling analysis for thin-walled composite beam under end moment", Engineering Structures, vol. 29, no. 8, pp. 1739-1751, 2007. [Online]. Available: https://doi.org/10.1016/j.engstruct.2006.09.017.

[3] T. P. Vo and J. Lee, "Geometrically nonlinear analysis of thin-walled composite box beams", Computers & Structures, vol. 87, no. 3-4, pp. 236-245, 2009. [Online]. Available: https://doi.org/10.1016/j.compstruc.2008.10.002.

[4] T. P. Vo and J. Lee, "Geometrically nonlinear analysis of thin-walled open-section composite beams", Computers & Structures, vol. 88, no. 5-6, pp. 347-356, 2010. [Online]. Available: https://doi.org/10.1016/j.compstruc.2009.11.007. ISSN: 0045-7949.

[5] N. Silvestre and D. Camotim, "First and second-order GBT for arbitrary orthotropic materials", Thin-Walled Structures, vol. 40, no. 9, pp. 755-820, 2002.

[6] N.M.F. Silva, N. Silvestre, and D. Camotim, "GBT formulation to analyze the buckling behavior of FRP composite open-section thin-walled columns", Composite Structures, vol. 93, pp. 79-92, 2010.

[7] C. Basaglia, D. Camotim, and N. Silvestre, "Global buckling analysis of plane and space thin-walled frames in the context of GBT", Thin-Walled Structures, vol. 46, pp. 79-101, 2008.

[8] C. M. Saravia, S. P. Machado, and V. H. Cortínez, "A geometrically exact nonlinear finite element for composite closed section thin-walled beams", Computers & Structures, vol. 89, no. 23-24, pp. 2337-2351, 2011. [Online]. Available: https://doi.org/10.1016/j.compstruc.2011.07.009.

[9] H. Ahmadi and H. A. Rasheed, "Lateral torsional buckling of anisotropic laminated thin-walled simply supported beams subjected to mid-span concentrated load", Composite Structures, vol. 185, pp. 348-361, Jan. 2018. [Online]. Available: https://doi.org/10.1016/j.compstruct.2017.11.027.

[10] S. Huang and P. Qiao, "Buckling of thin-walled I-section laminated composite curved beams", Thin-Walled Structures, vol. 154, article no. 106843, Sep. 2020. [Online]. Available: https://doi.org/10.1016/j.tws.2020.106843.

[11] S. Huang and P. Qiao, "Nonlinear stability analysis of thin-walled I-section laminated composite curved beams with elastic end restraints", Engineering Structures, vol. 226, article no. 111336, 2021. [Online]. Available: https://doi.org/10.1016/j.engstruct.2020.111336.

[12] D. Banić, G. Turkalj, and D. Lanc, "Stability analysis of shear deformable cross-ply laminated composite beam-type structures", Composite Structures, vol. 303, p. 116270, 2023. [Online]. Available: https://doi.org/10.1016/j.compstruct.2022.116270.

[13] I. Pešić and G. Turkalj, "Analiza izvijanja roštiljne konstrukcije metodom konačnih elemenata", Engineering Review, vol. 27, no. 1, pp. 39-47, 2007.

[14] G. Turkalj, J. Brnic, and J. Prpic Orsic, "Large rotation analysis of elastic thin-walled beam-type structures using ESA approach", Computers & Structures, vol. 81, pp. 1851-1864, 2003.

[15] D. Lanc, G. Turkalj, and I. Pesic, "Global buckling analysis model for thin-walled composite laminated beam type structures", Composite Structures, vol. 111, pp. 371-380, 2014. [Online]. Available: https://doi.org/10.1016/j.compstruct.2014.01.020.

[16] G. Turkalj, D. Lanc, J. Brnic, and I. Pesic, "A beam formulation for large displacement analysis of composite frames with semi-rigid connections", Composite Structures, vol. 134, pp. 237-246, 2015. [Online]. Available: https://doi.org/10.1016/j.compstruct.2015.08.068.

[17] B. A. Izzuddin, "Conceptual issues in geometrically nonlinear analysis of 3D framed structures", Computer Methods in Applied Mechanics and Engineering, vol. 191, pp. 1029-1053, 2001.

[18] D. Lanc, I. Pesic, and G. Turkalj, "Stability Analysis of Laminated Composite Thin-Walled Beam Structures", in Proceedings of the Eleventh International Conference on Computational Structures Technology, B.H.V. Topping, Ed., Civil-Comp Press, Stirlingshire, United Kingdom, 2012, paper 224, [Online]. Available: https://doi.org/10.4203/ccp.99.224

[19] D. Lanc, G. Turkalj, and I. Pešić, "Effect of shear flexibility in buckling analysis of beam structures", Machines, Technologies, Materials, vol. 7, pp. 58-61, 2015.

[20] I. Pešić, D. Lanc, and Goran Turkalj, "Non-linear thermal buckling analysis of thin-walled beam structures", Engineering Review, vol. 35, no. 3, pp. 239-245, 2015.

[21] I. Pešić, D. Lanc, and G. Turkalj, "Non-linear global stability analysis of thin-walled laminated beam-type structures", Computers & Structures, vol. 173, pp. 19-30, 2016. [Online]. Available: https://doi.org/10.1016/j.compstruc.2016.05.015.

[22] G. Turkalj, J. Brnic, and J. Prpic Orsic, "ESA formulation for large displacement analysis of framed structures with elastic–plasticity", Computers & Structures, vol. 82, pp. 2001-2013, 2004.

[23] J. E. B Cardoso, N. M. B. Benedito, A. J. J. Valido, “Finite element analysis of thin-walled composite laminated beams with geometrically nonlinear behavior including warping deformation”, Thin-Walled Structures, vol. 47, pp. 1363-1372, 2009.